



## Experimental Investigation of the Effect of Hybrid fibers on Lightweight Concrete Beams Reinforced with GFRP Bars

S. E. Vakili<sup>1</sup>, P. Homami<sup>1\*</sup>, M. R. Esfahani<sup>2</sup>

<sup>1</sup> Faculty of Engineering, Department of Civil Engineering, Kharazmi University, Tehran, Iran

<sup>2</sup> Faculty of Engineering, Department of Civil Engineering, Ferdowsi University of Mashhad, Mashhad, Iran

**ABSTRACT:** The main purpose of this study investigated the effects of hybrid use of micro glass fiber (GF), micro polypropylene fiber (PF) and macro steel fiber (SF) on the flexural capacity, energy absorption, ultimate load carrying, failure mode and ductility behavior of lightweight aggregate concrete (LWC) beams reinforced with glass fiber reinforced polymer (GFRP) bars. A total of eight beams with a rectangular cross-section and 100 mm wide  $\times$  200 mm deep  $\times$  1500 mm long, were cast and tested up to failure under four-point bending. The correction factor ( $\phi$ ) calculated compared with American design codes of ACI 440.1R-06 and ISIS design manual No. 3. The  $\phi$  factor for beams made of hybrid PF, SF into the LWC mixes (PSLWC) and reinforced with  $0.9 \rho_{fb}$ ; where  $\rho_{fb}$  is the balanced reinforcement ratio of the GFRP bars is approximately 1.38 times to the  $\phi$  factor for beams made of hybrid GF, PF into the LWC mixes (GPLWC) and hybrid GF, SF added into the LWC mixes (GSLWC) that reinforced with  $0.9 \rho_{fb}$ . The results experimental showed the ultimate load-carrying capacity increased 5% to 49%, with increasing reinforcement ratio from  $0.9 \rho_{fb}$  to  $1.4 \rho_{fb}$ . According to experimental observations, failure modes in the beams made of GPLWC, GSLWC and PSLWC also reinforced with  $0.9 \rho_{fb}$  failure modes coincides with the failure modes ACI 440.1R-06. The results indicate that the use of GPLWC, GSLWC and PSLWC at beams reinforced with GFRP bars improves the flexural capacity, ultimate load carrying, energy absorption and ductility.

### Review History:

Received: 18 December 2018

Revised: 20 January 2019

Accepted: 30 January 2019

Available Online: 30 January 2019

### Keywords:

Hybrid Fibers

Macro Steel Fiber

Micro Polypropylene and Glass Fiber

Lightweight Aggregate Concrete (LWC)

GFRP Bars

### 1- Introduction

The two main factors that can be used to stabilize concrete structures against earthquake and corrosion are the use of lightweight aggregate concrete (LWC) and glass fiber reinforced polymers (GFRP) bars in concrete structures. Recently, FRP composite materials-polymeric resin-embedded fibers- have become an alternative for reinforced concrete with steel fiber. Considering non-corrosive and non-magnetic properties of FRP materials, in FRP-reinforced concrete, the problems of steel bar corrosion and electromagnetic interference can be prevented [1]. Considering the numerous excellent advantages of LWC much attention has been paid to its development [2]. LWC is effectively utilized in the civil engineering field during many years, LWC involves many desired properties including better durability, superior thermal insulation, reduced density, better fire resistance, and superior seismic resistance compared with conventional concrete [3-7]. Adding fibers to LWC is an effective method for improving the mixture strength and toughness [8]. Among the different types of fibers, steel fiber or polypropylene fibers were widely applied [8, 10, 11]. The addition of fibers to the LWC significantly

increments its impact resistance, post-cracking ductility and flexural tensile strength and the effectiveness of high-performance polypropylene fibers on post-peak behavior was higher than its effectiveness on pre-peak behavior [12-15]. Crack width and large deflection of fiber-reinforced polymer (FRP) bar reinforced with concrete beams. Adding the steel fiber the density increases and the workability of plain LWC decreases. Incidentally, The interfacial transition zone between aggregates and paste was not the weakest link in steel fiber reinforced LWC (SFLWC) [16,17]. The capacity of energy absorption is increased by increasing the volume fraction of the fibers [18]. In this study is related to the status of knowledge of hybrid micro glass fiber (GF), micro polypropylene fiber (PF) and macro steel fiber (SF) on the flexural capacity, energy absorption, ultimate load carrying, failure mode and ductility behavior for beams made with LWC and reinforced with glass fiber reinforced polymers (GFRP) bars. Moreover, the results of evaluating the fiber lightweight expanded clay aggregate (LECA) concrete with mechanical tests are described and discussed in the current research. The present experimental study is emphasized on the researches of the flexural capacity, ultimate load carrying, energy absorption, failure mode and ductility behavior on the hybrid GF, PF were added

Corresponding author, E-mail: homami@khu.ac.ir

into the LWC mixes (GPLWC) and hybrid PF, SF were added into the LWC mixes (PSLWC) and hybrid PF, SF were added into the LWC mixes (PSLWC) beams reinforced with GFRP bars.

material properties were delivered by the manufacturer (Table 3). A naphthalene type superplasticizer was used in all mixtures to obtain sufficient fluidity.

**2- Experimental Program**

**2- 1- Materials**

The cement used in this study was 1-325 Portland cement composed ISIRI N.389 [19]. The specific gravity of 3.15 g/cm<sup>3</sup>. Micro-silica utilized in this study involved an apparent density of 2.2 g/cm<sup>3</sup>, the specific surface area of 2800 cm<sup>2</sup>/g. The lightweight expanded clay aggregate (LECA) utilized in this study (Figure 1) and also Fine aggregate included crushed sand with a nominal maximum size of 5.0 mm and a bulk density of 1560 kg/m<sup>3</sup> (Table 1). Properties of GF, PF, and SF (Figure 2) provided by the manufacturer are represented in Table 2. The GFRP bars were provided by the manufacturer (Figure 3) and their



**Figure 1. Light expanded clay aggregate (LECA)**

**Table 1. Properties of aggregates**

| Aggregates                           | Size (mm)  | Apparent density (kg/m <sup>3</sup> ) | Water absorption (%) |       |
|--------------------------------------|------------|---------------------------------------|----------------------|-------|
|                                      |            |                                       | 1 h                  | 24 h  |
| Light Expanded Clay aggregate (LECA) | 1- 9.50    | 1300                                  | 8.60                 | 11.10 |
| Sand                                 | 0.15- 4.75 | 2660                                  | 0.35                 | 0.80  |

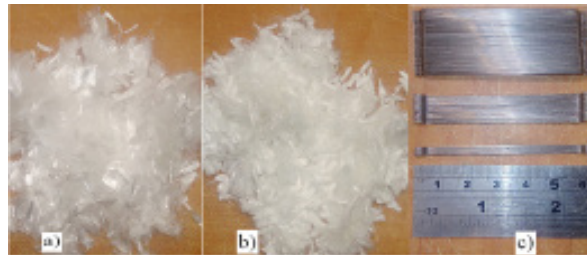


**Figure 2. Fibers used in this study: a) macro fiber steel, b) microfiber polypropylene and c: microfiber Glass**

**Table 2. Properties of fibers**

| Fiber type    | Length (mm) | Diameter (mm) | Aspect ratio (l/d) | Density (g/cm <sup>3</sup> ) | Tensile Strength (GPa) | Geometry    |
|---------------|-------------|---------------|--------------------|------------------------------|------------------------|-------------|
| Steel         | 60          | 0.90          | 66.66              | 7.80                         | 3.0                    | End hooked  |
| Polypropylene | 12          | 0.023         | 521.73             | 0.91                         | 0.40                   | Fibrillated |
| Glass         | 15          | 0.019         | 789.47             | 2.60                         | 1.50                   | Fibrillated |

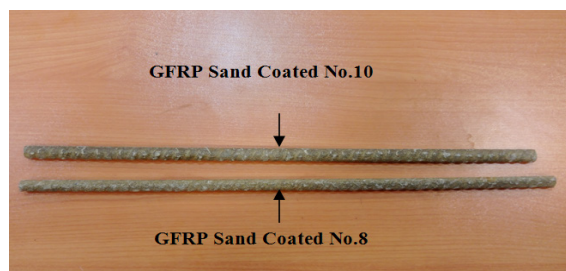


**Figure 3. GFRP bars used in this study**

**Table 3. Material Properties of the GFRP bars**

| Type | Diameter (mm) | Area* (mm <sup>2</sup> ) | EL* (GPa) | F* <sub>1</sub> (kN) | F* <sub>2</sub> (kN) | ε* <sub>1</sub> (mm)    | ε* <sub>2</sub> (mm)   |
|------|---------------|--------------------------|-----------|----------------------|----------------------|-------------------------|------------------------|
| GFRP | 8             | 506.7                    | 49.4      | 30.0                 | 12.0                 | 10.38×10 <sup>-3</sup>  | 3.04 ×10 <sup>-3</sup> |
| GFRP | 10            | 791.7                    | 51.0      | 33.1                 | 11.9                 | 11.277×10 <sup>-3</sup> | 2.98×10 <sup>-3</sup>  |

Area\*: cross-sectional area of specimen, EL\*: axial (longitudinal) modulus of elasticity, F\*<sub>1</sub> and ε\*<sub>1</sub>: load and corresponding strain, respectively, F\*<sub>2</sub> and ε\*<sub>2</sub>: load and corresponding strain, respectively, at approximately 20% of the ultimate tensile capacity, respectively.

### 2- 2- Mixture proportions and production

Table 4, represents the mixture proportions. The mixing procedure was completed by initially transferring the dry aggregate to the mixer and mixing it for 30 s. Then, half of the water plus the total superplasticizer were combined and added to the mixture and mixed for 30 s. Then, the cement was added to one-third of the fiber, the micro-silica was mixed with half of the water and a gel was obtained. Subsequently, it was added to the mixture and for 3 min was mixed. The hybrid GF and PF the content 0.3% volume of concrete and 0.80% volume of concrete added to LWC mix (GFLWC), respectively. The hybrid

GF and SF the content 0.3 vol% and 0.25 vol%, added to LWC mix (GSLWC) respectively and hybrid PF and SF the content 0.8 vol% and 0.25 vol%, added to LWC mix (PSLWC) respectively used in the specimens according to the Table 4.

### 3- Test methods

#### 3- 1- Slump tests

To determine the workability of fresh LWC, GPLWC, GSLWC and PSLWC mixtures (Table 5), the slump tests were conducted based on ASTM-C143 [20].

**Table 4. Mixture proportions of LWC, GPLWC, GSLWC and PSLWC**

| Name of specimen | Cement (kg/m <sup>3</sup> ) | Water (kg/m <sup>3</sup> ) | Sand (kg/m <sup>3</sup> ) | LECA (kg/m <sup>3</sup> ) | Micro silica (kg/m <sup>3</sup> ) | Super plasticizer (kg/m <sup>3</sup> ) | Fiber volume fraction (%) |      |      |
|------------------|-----------------------------|----------------------------|---------------------------|---------------------------|-----------------------------------|--|---------------------------|------|------|
|                  |                             |                            |                           |                           |                                   |  | GF                        | PF   | SF   |
| LWC              | 500                         | 195                        | 265                       | 685                       | 15                                | 5                                      | 0                         | 0    | 0    |
| GPLWC            | 500                         | 195                        | 265                       | 685                       | 15                                | 5                                      | 0.30                      | 0.80 | 0    |
| GSLWC            | 500                         | 195                        | 265                       | 685                       | 15                                | 5                                      | 0.30                      | 0    | 0.25 |
| PSLWC            | 500                         | 195                        | 265                       | 685                       | 15                                | 5                                      | 0                         | 0.80 | 0.25 |

**Table 5. Results of compressive strength, oven-dry density and slump tests for specimen LWC, GPLWC, GSLWC and PSLWC**

| Name of specimen | F <sub>cu</sub> (MPa) | Oven dry density (kg/m <sup>3</sup> ) | Slump (mm) |
|------------------|-----------------------|---------------------------------------|------------|
| LWC              | 35                    | 1530                                  | 100        |
| GPLWC            | 34                    | 1565                                  | 70         |
| GSLWC            | 44                    | 1680                                  | 55         |
| PSLWC            | 36                    | 1588                                  | 65         |

### 3- 2- Mechanical properties

For saving time all the mechanical property tests were performed for 28 days. Table 5 indicates the compressive strength results along with the oven density. Based on BS 1881-116 [21]. For each mixture proportion, three 150 mm × 150 mm × 150 mm cube samples were prepared for the compressive strength test. Using hydraulic pressure testing machine with a maximum load capacity of 2000 kN, the compressive load was implemented.

### 4- Test Setup and Procedure

The specimens were tested under the four-point bending, with a length of 1500 mm, a depth of 200 mm, a width of 100 mm and a shear span of 550 mm. The distance

between point loads was 300 mm. All the beams had a 50 mm overhang on each side. Two FRP bars were utilized in the lower part (bottom reinforcement) of each beam; these bars were GFRP bars with diameters of 8 or 10 mm. Hence, approximately, the effective depths of the beams with the #8 and #10 mm bars were 170 mm (concrete cover was 30 mm). One steel bar was utilized in the upper part (top reinforcement) and the φ6@7.5cm steel stirrups were used along 55 cm at each end of the beams. Furthermore, in the middle part of beams, φ6@15cm steel stirrups were used. Totally, eight beams were constructed with different flexural reinforcement ratios. Details and designations of the beams are presented in Figure 4 and Table 6, respectively. To investigate the flexural

performance of GPLWC, GSLWC and PSLWC concrete beams reinforced with GFRP bars, the four-point static

bending test was employed. Figure 5 represents the test setup and schematic diagram.

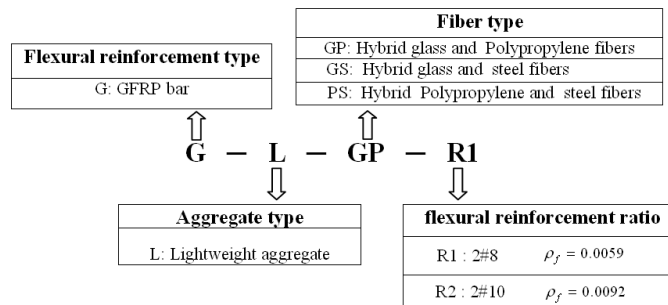
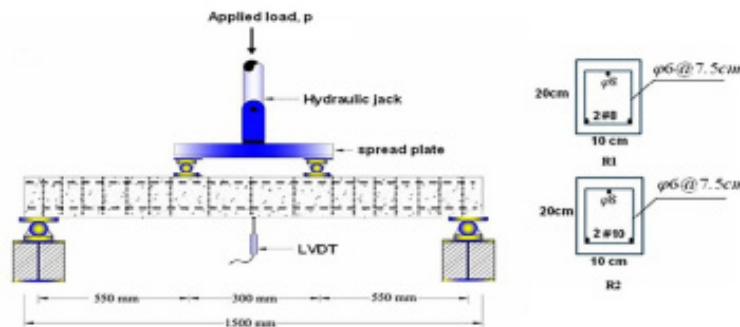


Figure 4. Designation of the test beams



(a) Actual test setup



(b) The schematic test set up and two different types of the beam section

Figure 5. Schematic of the four-point static bending test

Table 4. Mixture proportions of LWC, GPLWC, GSLWC and PSLWC

| Beam code | Beam dimensions |            | Effective span<br>L (mm) | Bottom Reinforcement<br>(GFRP bars) | Top Reinforcement<br>(steel bar) | Stirrups<br>(steel) |
|-----------|-----------------|------------|--------------------------|-------------------------------------|----------------------------------|---------------------|
|           | width b (mm)    | Depth (mm) |                          |                                     |                                  |                     |
| G-L-R1    | 100             | 200        | 1400                     | 2#8                                 | 1φ8                              | φ6@7.5cm            |
| G-L-R2    | 100             | 200        | 1400                     | 2#10                                | 1φ8                              | φ6@7.5cm            |
| G-L-GP-R1 | 100             | 200        | 1400                     | 2#8                                 | 1φ8                              | φ6@7.5cm            |
| G-L-GP-R2 | 100             | 200        | 1400                     | 2#10                                | 1φ8                              | φ6@7.5cm            |
| G-L-GS-R1 | 100             | 200        | 1400                     | 2#8                                 | 1φ8                              | φ6@7.5cm            |
| G-L-GS-R2 | 100             | 200        | 1400                     | 2#10                                | 1φ8                              | φ6@7.5cm            |
| G-L-PG-R1 | 100             | 200        | 1400                     | 2#8                                 | 1φ8                              | φ6@7.5cm            |
| G-L-PG-R2 | 100             | 200        | 1400                     | 2#10                                | 1φ8                              | φ6@7.5cm            |



**5- Test results and discussion**

In this section, the experimental results are summarized including the failure mode, load-deflection behavior, ductility, flexural capacity and energy absorption of the tested beams.

**5- 1- Mode of failure**

The results showed that, For LWC beams without hybrid fibers when the reinforcement ratio is less than the balanced ratio ( $0.9 \rho_{fb}$ ) or more than the balanced ratio ( $1.4 \rho_{fb}$ ) failure mode of crush concrete occurred. For hybrid fibers, LWC beams when the reinforcement ratio is less than the balanced ratio ( $0.9 \rho_{fb}$ ) failure mode of GFRP rupture (GR) and when the reinforcement ratio is more than balanced ratio ( $1.4 \rho_{fb}$ ) crush concrete (CC) occurred. The failure mode for hybrid fibers LWC beams reinforced with GFRP bars is in accordance with the ACI 440.1R-06. The observed failure modes of the tested beams are presented in Table 7. The final situation of the

beams constructed by the LWC is indicated in Figure 6. The final situation of the GPLWC, GSLWC, and PSLWC samples are illustrated in Figures 7 to 9, respectively. Based on Figures 6, 7b, 8b and 9b, the concrete crushing (CC) failure mode in the compression zone appeared for the LWC, GPLWC, GSLWC and PSLWC. It should be mentioned that this failure mode was recommended by the ACI440.1R-06 code for any concrete beams reinforced with FRP bars since this kind of failure is more gradual, less brittle and less catastrophic with higher deformability in comparison with the tensile rupture of FRP bars [22, 23]. According to Figures 7a, 8a and 9a presenting the GFRP rupture (GR) failure mode, it is indicated that in G-L-GP-R1, G-L-GS-R1 and G-L-PS-R1 beams the failure mode of GPLWC, GSLWC and PSLWC from CC to the GR was changed due to an increase in balanced reinforcement ratio of the GFRP bars ( $0.9 \rho_{fb}$ ) from 0.9 to 1.4.

**Table 7. Test results and failure modes**

| Beam code | Reinforcement ratio ( $\rho_f / \rho_{fb}$ )% | Ultimate load $P_{exp}$ (kN) | Mid-Span (mm) | Failure Modes | ACI failure consistency |
|-----------|---|------------------------------|---------------|---------------|-------------------------|
| G-L-R1    | 0.9   | 18.62                        | 16.64         | C.C           | -                       |
| G-L-R2    | 1.4   | 27.46                        | 14.50         | C.C           | ✓                       |
| G-L-GP-R1 | 0.9   | 32.86                        | 52.53         | G.R           | ✓                       |
| G-L-GP-R2 | 1.4   | 35.80                        | 29.11         | C.C           | ✓                       |
| G-L-GS-R1 | 0.9   | 33.84                        | 33.74         | G.R           | ✓                       |
| G-L-GS-R2 | 1.4   | 50.52                        | 40.35         | C.C           | ✓                       |
| G-L-PS-R1 | 0.9   | 38.26                        | 46.34         | G.R           | ✓                       |
| G-L-PS-R2 | 1.4   | 47.08                        | 44.13         | C.C           | ✓                       |

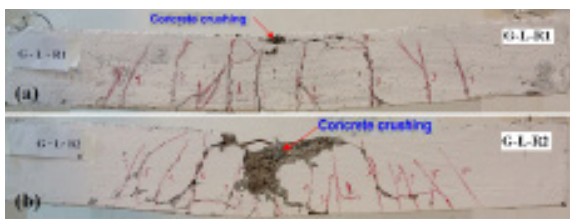


**Figure 6. Modes of failure in the specimens G-L-R1, G-L-R2: (a) Concrete crushing failure in the specimen G-L-R1, (b) Concrete crushing failure in the specimen G-L-R2**

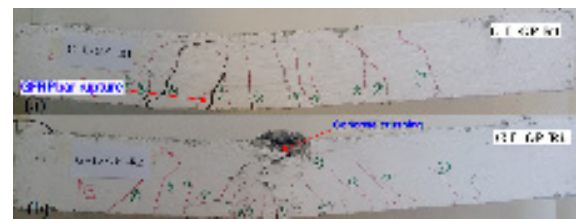


**Figure 7. Modes of failure in the specimen L-GP-R1, G-L-GP-R2: (a) Rupture of GFRP reinforcement bars in the specimen G-L-GP-R1, (b) Concrete crushing failure in the specimen G-L-GP-R2**

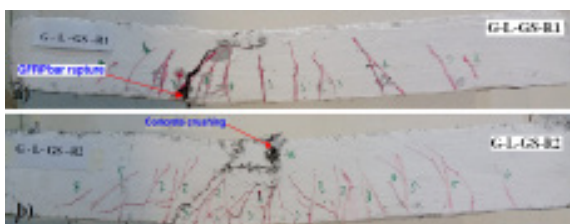


**Figure 8. Modes of failure in the specimens G-L-GS-R1, G-L-GS-R2: (a) Rupture of GFRP reinforcement bars in the specimen G-L-GS-R1, (b) Concrete crushing failure in the specimen G-L-GS-R2**



**Figure 9. Modes of failure in the specimens G-L-PS-R1, G-L-PS-R2: (a) Rupture of GFRP reinforcement bars in the specimen G-L-PS-R1, (b) Concrete crushing failure in the specimen G-L-PS-R2**

### 5- 2- Load-deflection behavior

Table 7 and Figures 10 and 11 provide the experimental load to mid-span deflection curves and ultimate loads of the GFRP reinforced LWC, GPLWC, GSLWC, and PSLWC beams. Each curve in dictates the deflection obtained by the LVDT at beam mid-span. The behavior of the un-cracked beams is represented in the first part of the curves up to the first cracking. The corresponding force is the first crack in the beams are shown in Figure 12. The amount of force that creates the first cracks in the beams as seen in the figure the amount of force that the first cracks in the beam create are increased by adding fiber to LWC. In all beams made with hybrid fibers, the amount of cracking force is greater than the non-fiber beam the increase in the amount force with adding hybrid GF with SF, hybrid GF with PF and hybrid PF with SF is 47-64%, 36-57% and 40-60% respectively. Adding fibers

due to of the bridging between the micro-cracks will delay cracking the presence of fibers in LWC also increases the tensile strength of concrete, which is directly related to the appearance of the first crack in the beam. The second part deals with the behavior of the cracked beams with reduced stiffness. As it is observed, added fibers led to a significant increment in the ductility of the beams, which were reinforced by  $1.4 \rho_{fb}$  GFRP bars. Figures 10a, 10b, and 10c represent the effect of hybrid fibers LWC reinforcement ratio of  $0.9 \rho_{fb}$  for G-L-GP-R1, G-L-GS-R1 and G-L-PS-R1 beams in comparison with the G-L-R1 beam that reinforcement ratio of  $0.9 \rho_{fb}$  increases the ultimate load by 76%, 82% and 105%, respectively. Figs. 10e, 10f, and 10g indicate the effect of hybrid fibers LWC reinforcement ratio of  $1.4 \rho_{fb}$  for the G-L-GP-R2, G-L-GS-R2, and G-L-PS-R2 beams compared to the G-L-R2 beam in that reinforcement ratio of  $1.4 \rho_{fb}$  increases the ultimate load by 30%, 84% and 71%, respectively.

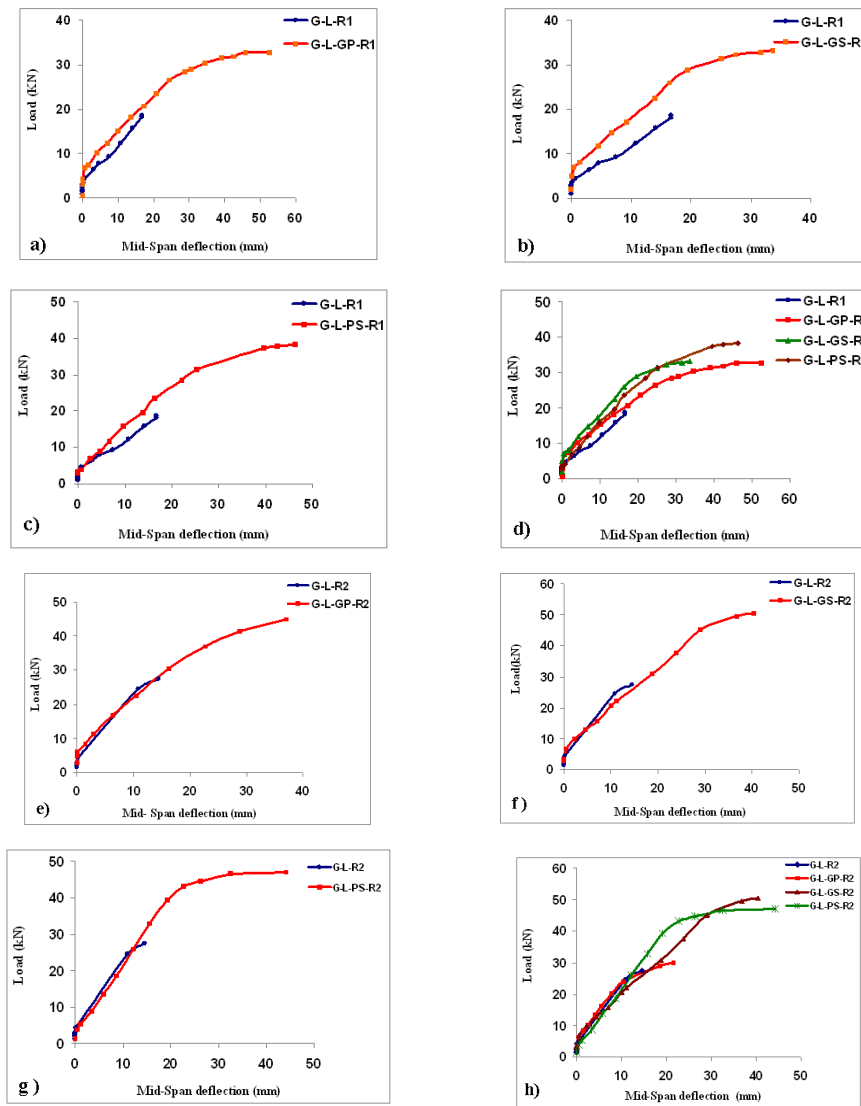


Figure 10. Load-mid-span deflections: (a) Beam code: G-L-R1 and G-L-GP-R1; (b) Beam code: G-L-R1 and G-L-GS-R1; (c) Beam code: G-L-R1 and G-L-PS-R1; (d) Beam code: G-L-R1, G-L-GP-R1, G-L-GS-R1, and G-L-PS-R1; (e) Beam code: G-L-R2 and G-L-GP-R2; (f) Beam code: G-L-R2 and G-L-GS-R2; (g) Beam code: G-L-R2 and G-L-PS-R2; (h) Beam code: G-L-R2 and G-L-GP-R2

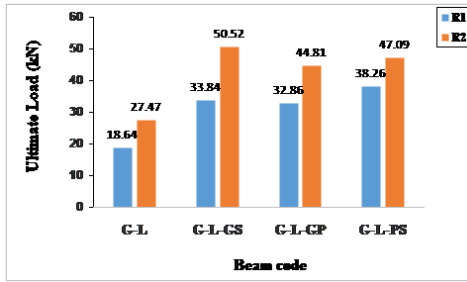


Figure 11. Ultimate load

5- 3- Ductility

Figure 10d in dictates that adding hybrid fibers to the LWC can significantly increase the ductility in comparison to the specimens without added fibers. Ductility G-L-GP-R1, G-L-PS-R1, and G-L-GS-R1 beams increase to 2.27, 2.33 and 2.74, respectively. Figure 10 represents the increase in the ductility of the G-L-GP-R2, G-L-PS-R2 and G-L-GS-R2 beams to 2.44, 2.99 and 3.33, respectively.

5- 4- Flexural capacity

The flexural capacity of an FRP reinforced member relies on whether the failure is controlled by CC or FRP rupture modes [18]. By ACI 440.1R-06 and ISIS design manual No. 3 [24] failure modes of the beams and their nominal flexural strength can be determined and compared with the test results represented in Table 7. ACI 440.1R-06 and ISIS design manual No. 3 are provided for pure LWC and

they do not involve any comments for fiber added LWC. The correction factor ( $\phi$ ) obtained from the comparison experimental results with ACI 440.1R-06 and ISIS design manual No. 3 are provided for pure LWC and they do not involve any comments for fiber added LWC. Thus, for matching the nominal calculated strength of the code (for pure LWC) with the experimental results (for the fiber added LWC), factor ( $\phi$ ) calculated a strength factor for the flexure capacity ( $\phi$ ). Table 8 represents the results of  $\phi$  factor for different added hybrid fibers materials matching to the design codes. As it is observed, the ratio of ( $M_{exp}$ : Experimental Flexural capacity,  $M_{ACI}$ : nominal flexural strength (ACI 440.1R-06) is less than 1 for the five G-L-R1 to G-L-R2, G-L-GP-R2 beams and also ratio of  $M_{exp}$  to ( $M_{ISIS}$ : nominal flexural strength (ISIS design manual No. 3) is less than 1 for three G-L-R1, G-L-R2 and G-L-GP-R2 beams.

5- 5- Energy absorption capacity

The energy absorption capacities of the beams were calculated as the area surrounded by the load-deflection curve. The energy absorption capacity of all eight beams is represented in Figure 10. It is shown in Figure 13 that the beams made with added fiber LWC involve much more energy absorption capacity than the pure LWC beams. The capacities of the specimens of G-L-GP-R1, G-L-GS-R1 and G-L-PS-R1 are respectively, 5.25, 4.80 and 3.45, times higher compared to the capacity of G-L-R1 while the capacities of the G-L-GP-R2, G-L-GS-R2 and G-L-PS-R2 specimens are respectively, 6.70, 4.83 and 3.70, times higher compared to the capacity of G-L-R2.

Table 8. Comparisons between the nominal flexural strength calculated by design codes for pure LWC and the experimental capacities of the fiber added LWC

| Beam code | $M_{exp}$ (kNm) | $M_{n_{ACI}}$ (kNm) | $M_{n_{ISIS}}$ (kNm) | $\phi$                    |                            |
|-----------|-----------------|---------------------|----------------------|---------------------------|----------------------------|
|           |                 |                     |                      | $(M_{exp} / M_{n_{ACI}})$ | $(M_{exp} / M_{n_{ISIS}})$ |
| G-L-R1    | 5.12            | 7.41                | 6.12                 | 0.69                      | 0.84                       |
| G-L-R2    | 7.55            | 11.81               | 11.84                | 0.64                      | 0.64                       |
| G-L-GP-R1 | 9.04            | 7.41                | 6.12                 | 1.22                      | 1.47                       |
| G-L-GP-R2 | 12.32           | 11.80               | 11.84                | 1.04                      | 1.04                       |
| G-L-GS-R1 | 9.30            | 7.41                | 6.12                 | 1.25                      | 1.52                       |
| G-L-GS-R2 | 13.89           | 11.81               | 11.84                | 1.17                      | 1.17                       |
| G-L-PS-R1 | 10.51           | 7.41                | 6.12                 | 1.42                      | 1.71                       |
| G-L-PS-R2 | 12.95           | 11.81               | 11.84                | 1.09                      | 1.09                       |

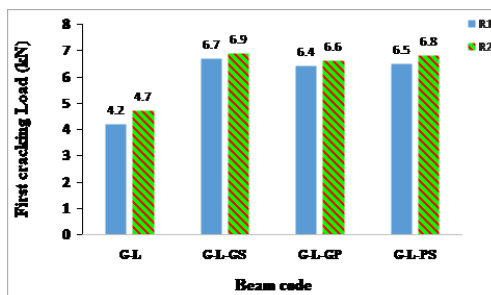


Figure 12. First cracking load

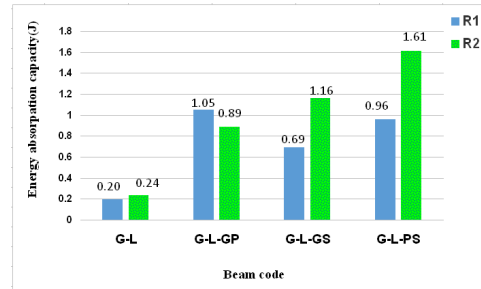


Figure 13. Energy absorption capacity of beams under static loading

## 6- Conclusions

In this study the load-deflection behavior, flexural capacity failure mode, ductility and energy absorption for were investigated for specimen beams made with lightweight aggregate concrete (LWC), hybrid micro glass fiber (GF) and micro polypropylene (PF) in the LWC (GPLWC), hybrid GF and macro steel fiber (SF) in the LWC (GSLWC) and hybrid PF and SF in the LWC (PSLWC) that reinforced with glass fiber reinforced polymer (GFRP) bars. The following remarks can be concluded from the present work:

- The use of hybrid fibers in the LWC beams reinforced by GFRP bars the failure mode is GFRP rupture governed when the balanced ratio was higher the reinforcement ratio and failure mode consistent with the ACI 440.1R-06.
- For specimen beams made with LWC, GPLWC, GSLWC, and PSLWC with a reinforcement ratio of  $0.9\rho_{fb}$  to  $1.4\rho_{fb}$ , the ultimate loads incremented up to 47%, 36%, 49% and 23%, respectively.
- Adding hybrid GF and SF in the LWC, hybrid GF and PF in the LWC and hybrid PF and SF in the LWC can significantly increase in the amount force corresponding to the first cracking 47-64%, 36-57% and 40-60% respectively.
- Adding hybrid fibers to the LWC can significantly increase the ductility in comparison to the specimens without added fibers. For specimen beams made with GPLWC, PSLWC and GSLWC reinforced with  $0.9\rho_{fb}$ , ductility increased by 2.27, 2.33 and 2.74, respectively and increased up to 2.44, 2.99 and 3.33, respectively, times for specimen beams made with GPLWC, PSLWC and GSLWC and reinforced with  $1.4\rho_{fb}$ , respectively.
- Flexural capacity matching factor ( $\phi$ ) calculated from  $M_{exp}/M_{nACI}$  indicated the efficiency of the hybrid fibers added to the LWC material. The  $\phi$  factor for beams made with PSLWC and reinforced with  $0.9\rho_{fb}$  is approximately 1.16 times to the  $\phi$  factor for beams made with GPLWC and GSLWC that reinforced with  $0.9\rho_{fb}$ .
- Flexural capacity matching factor ( $\phi$ ) calculated from  $M_{exp}/M_{nISIS}$  represented the efficiency of the hybrid fibers added to the LWC material. The  $\phi$  factor for beams made with PSLWC and reinforced with  $0.9\rho_{fb}$  is almost 1.14 times to the  $\phi$  factor for beams made with GPLWC and GSLWC that reinforced with  $0.9\rho_{fb}$ .
- Energy absorption increased by adding fibers into the LWAC material. The best results were obtained for specimens GPLWAC reinforced with  $0.9\rho_{fb}$  and specimen PSLWC reinforced with  $1.4\rho_{fb}$  which was 5.25 and 6.70 times greater than beams without added fibers, respectively.

## References

- [1] Committee, A. (2006). "Guide for the design and construction of structural concrete reinforced with FRP bars." 440.1 R.
- [2] Shafiq, P., et al. (2011). "A new method of producing high strength oil palm shell lightweight concrete." Materials & Design 32(10): 4839-4843.
- [3] Ma, H., et al. (2013). "Study on mechanical properties of steel fiber reinforced autoclaved lightweight shell-aggregate concrete." Materials & Design (1980-2015) 52: 565-571.
- [4] Oktay H., et al. (2015). "Mechanical and thermophysical properties of lightweight aggregate concretes." Constr. Build. Mater. 96: 217-225.
- [5] Soner G., (2018). "The effect of polyamide fibers on the strength and toughness properties." Constr. Build. Mater. 173: 394-402.
- [6] Bogas, J. A. and A. Gomes (2015). "Non-steady-state accelerated chloride penetration resistance of structural lightweight aggregate concrete." Cement and Concrete Composites 60: 111-122.
- [7] Bilodeau, A., et al. (2004). "Optimization of the type and amount of polypropylene fibres for preventing the spalling of lightweight concrete subjected to hydrocarbon fire." Cement and Concrete Composites 26(2): 163-174.
- [8] Libre, N. A., et al. (2011). "Mechanical properties of hybrid fiber reinforced lightweight aggregate concrete made with natural pumice." Construction and Building Materials 25(5): 2458-2464.
- [9] Campione G., and L. La Mendola, (2004). "Behavior in compression of lightweight fiber reinforced concrete confined with transverse steel reinforcement." Cem. Concr. Compos. 26(6): 645-656.
- [10] Domaga-a, L. (2011). "Modification of properties of structural lightweight concrete with steel fibers." Journal of Civil Engineering and Management 17(1): 36-44.
- [11] Chen, B. and J. Liu (2005). "Contribution of hybrid fibers on the properties of the high-strength lightweight concrete having good workability." Cement and Concrete Research 35(5): 913-917.
- [12] Li, J., et al. (2017). "Comparison of flexural property between high performance polypropylene fiber reinforced lightweight aggregate concrete and steel fiber reinforced lightweight aggregate concrete." Construction and Building Materials 157: 729-736.
- [13] Qian, C. and P. Stroeven (2000). "Development of hybrid polypropylene-steel fiber-reinforced concrete." Cement and Concrete Research 30(1): 63-69.
- [14] Khaloo, A., et al. (2014). "Mechanical performance of self-compacting concrete reinforced with steel fibers." Construction and Building Materials 51: 179-186.
- [15] Hamoush, S., et al. (2010). "Deflection behavior of concrete beams reinforced with PVA micro-fibers." Construction and Building Materials 24(11): 2285-2293.
- [16] Zhu, H., et al. (2018). "Flexural behavior of partially fiber-reinforced high-strength concrete beams reinforced with FRP bars." Construction and Building Materials 161: 587-597.
- [17] Jun Li, J., et al. (2017). "Investigation on flexural toughness evaluation method of steel fiber reinforced



- lightweight aggregate concrete.” *Construction and Building Materials* 131: 449-458.
- [18] Lee J.-H., et al., (2017). “Flexural capacity of fiber reinforced concrete with a consideration of concrete strength and fiber content” *Constr. Build. Mater.* 138: 222-231.
- [19] Iran), I. I. o. S. a. I. R. o. (2000). “Specification for Portland cement.” ISIRI Number 389.
- [20] Standard, A. (2015). “Standard Test Method for Slump of Hydraulic-Cement Concrete.” *ASTM Annual Book of ASTM Standards*.
- [21] Standard, BS. (1983). “Method for determination of compressive strength of concrete cubes concrete specimens.” BS 1881-116:1983.
- [22] Taly, N., et al. (2006). *Reinforced concrete design with FRP composites*, CRC press.
- [23] Kakizawa, T., et al. (1993). “Flexural behavior and energy absorption of carbon FRP reinforced concrete beams.” *Special Publication 138*: 585-598.
- [24] Canada, Intelligent Sensing for Innovative Structures (ISIS), (2007). “Design Manual No. 3. Reinforcing concrete structures with fiber reinforced polymers.”

Please cite this article using:

S. E. Vakili, P. Homami, M. R. Esfahani, Experimental Investigation of the Effect of Hybrid fibers on Lightweight Concrete Beams Reinforced with GFRP Bars, *AUT J. Civil Eng.*, 3(2) (2019) 233-242.

DOI: 10.22060/ajce.2019.15474.5542



